# Detrital magnetite and chromite in Jack Hills quartzite cobbles: Further evidence for the preservation of primary magnetizations and new insights into sediment provenance

Matthew S. Dare [a], John A. Tarduno [a,b,*,1], Richard K. Bono [a], Rory D. Cottrell [a], James S. Beard [c], Kenneth P. Kodama [d]

[a] *Department of Earth and Environmental Sciences, University of Rochester, Rochester, NY, 14627, USA*
[b] *Department of Physics and Astronomy, University of Rochester, Rochester, NY, 14627, USA*
[c] *Virginia Museum of Natural History, Martinsville, VA, 24112, USA*
[d] *Department of Earth and Environmental Sciences, Lehigh University, Bethlehem, PA, 18015, USA*

## A B S T R A C T

The magnetization of zircons from sedimentary rocks of the Jack Hills (Yilgarn Craton, Western Australia) provide evidence for a Hadean to Paleoarchean geodynamo, 4.0 to 4.2 billion years old. These magnetizations pass a microconglomerate test, attesting to the fidelity of Jack Hills zircons as recorders of these most ancient magnetic signals. The lack of pervasive remagnetization of the Jack Hills is also documented through a positive conglomerate test conducted on cobble-sized clasts. A key element of the latter test is the preservation of a high unblocking temperature magnetization that can survive peak metamorphic temperatures. Rock magnetic studies suggest the mineral carrier is magnetite. Herein, we investigate the magnetic mineral carriers in cobble samples through scanning electron microscope and microprobe analyses, conduct an inter-laboratory paleomagnetic study to evaluate sensitivities required to evaluate the weak magnetizations carried by the Jack Hills sediments, and assess provenance information constrained by the opaque minerals. These data confirm magnetite as a detrital phase and the presence of high unblocking temperature magnetizations, further supporting the posit that the Jack Hills sediments can preserve primary magnetic signatures. We note that some of these magnetizations are near the measurement resolution of standard cryogenic magnetometers and thus exacting laboratory procedures are required to uncover these signals. In addition to magnetite, the cobbles contain an assemblage of Mg poor Cr–Fe chromites, Ni-sulfides and pyrrhotite that suggest a source in a layered intrusion different from the granitoid source of the zircons. Any Hadean rock fragment in these sediments, if present, remains elusive.

## 1. Introduction

The Jack Hills (JH) of Western Australia contain the oldest known terrestrial zircons, which are nearly 4.4 billion years old (Wilde et al., 2001; Valley et al., 2014). Studies using single silicate crystal paleointensity (SCP) techniques (Tarduno et al., 2006, 2007) suggest that some of these zircons record a geodynamo that is 4 billion years old, and perhaps older than 4.2 billion years old (Tarduno et al., 2015). The accuracy of this magnetic history is predicated on the preservation of a primary magnetization in the Jack Hills meta-sediments, which have seen metamorphic reheating of 420 to 475 °C at ~2.6 Ga (Rasmussen et al., 2010, 2011). A "microconglomerate" test, in which the paleomagnetic directions from oriented zircons were measured, provides evidence that the magnetizations can see through later metamorphic events. Specifically, the microconglomerate test was conducted on ~500–800 μm samples, each centered on a single large (200–300 μm) zircon (Tarduno et al., 2015). These measurements required the use of the ultra-high resolution 3-component DC SQUID magnetometer at the University of Rochester; this instrument offers an order of magnitude greater sensitivity than other high-resolution SQUID rock magnetometers. Thermal demagnetization using a $CO_2$ laser, which allows heating on short time scales that limit alteration (Tarduno et al., 2007), showed a characteristic remanent magnetization between 565 and 580 °C, carried by magnetic inclusions

in the zircons. While the characteristic remanent magnetizations from individual samples were well-defined (generally by 4 heating steps), the ensemble of directions could not be distinguished from a random distribution, indicating a positive microconglomerate test.

The possibility of the preservation of primary magnetization by the JH sediments was also supported by a paleomagnetic study of cobble-sized quartzite clasts (Tarduno and Cottrell, 2013). Thermal demagnetization, using a conventional ASC Scientific TD-48 thermal demagnetization oven, and measurement using a 2G Enterprises 755 3-component DC SQUID magnetometer with high resolution sensing coils, yielded a characteristic remanent magnetization at high unblocking temperatures ($>550\,°C$) indicative of a magnetite carrier. The presence of magnetite was further indicated by the observation of the Verwey transition (Verwey, 1939) – the crystallographic change from the monoclinic to the cubic phase in magnetite – in magnetic susceptibility versus temperature data.

The characteristic remanent magnetization from the cobbles also passed a conglomerate test indicating that a primary magnetization could be retained at high unblocking temperatures in the Jack Hills sediments. This observation can be further examined versus theoretical predictions of the influence of metamorphic reheating using Néel (1949, 1955) theory for single domain for thermoremanent magnetization. Specifically, the thermal relaxation time can be related to rock magnetic parameters as follows (Dunlop and Özdemir, 1997):

$$\frac{1}{\tau} = \frac{1}{\tau_0} exp\left[-\frac{\mu_0 V M_s H_K}{2kT}\left(1 - \frac{|H_0|}{H_K}\right)^2\right] \tag{1}$$

where $\tau_0$ ($\sim 10^{-9}$ s) is the interval between thermal excitations, $\mu_0$ is the permeability of free space, $V$ is grain volume, $M_s$ is spontaneous magnetization, $H_K$ is the microscopic coercive force, $k$ is Boltzmann's constant, $T$ is temperature, and $H_0$ is the applied field. This formulation was used by Pullaiah et al. (1975) to determine time-temperature relationships that can be in turn used to predict how secondary magnetizations might be acquired:

$$\frac{T_A ln(\tau_A/\tau_0)}{M_s(T_A)H_K(T_A)} = \frac{T_B ln(\tau_B/\tau_0)}{M_s(T_B)H_K(T_B)} \tag{2}$$

where the two relaxation times ($\tau_A$, $\tau_B$) correspond to temperatures ($T_A$, $T_B$) respectively, and $H_K >> H_0$. Equation (2) describes the tendency for the maximum metamorphic temperature to leak to a higher unblocking temperature range (Dunlop and Buchan, 1977; Dunlop, 1981). If we consider a peak metamorphic temperature of $420\,°C$, the lower bound constrained by the monazite-xenotime thermometry of Rasmussen et al. (2011), and a nominal reheating duration of 1 million years, SD unblocking temperatures up to $\sim 470\,°C$ could be affected. The upper bound on metamorphic reheating ($475\,°C$) with the same duration, suggests that SD unblocking temperatures up to $\sim 530\,°C$ could be affected. A heating duration of 10 m.y. would result in an increase in these upper temperature bounds by only $\sim 10\,°C$. These temperature estimates are in agreement with the sharp break seen in demagnetization data at high unblocking temperatures, and the start of the definition of a characteristic remanent magnetization.

Recently Weiss et al. (2015) reported on a study which in part sought to resample the cobble-bearing conglomerate bed study investigated by Tarduno and Cottrell (2013). GPS coordinates suggest that the stratigraphic horizons studied by Weiss et al. (2015) differ from the one sampled by Tarduno and Cottrell (2013), but some samples may be within 30–40 m of stratigraphic distance. Weiss et al. (2015) interpret their data as indicating either failed or indeterminate field tests; they conclude that the Jack Hills rocks were pervasively remagnetized in a single magnetic direction at ca. 1070 Ma (Wingate et al., 2002), and that magnetite as reported by

Tarduno and Cottrell (2013) from magnetic measurements is not intrinsic to the samples but is instead a product of laboratory alteration. There are several problems with these interpretations:

1. Weiss et al. (2015) were unable to isolate magnetizations from the critical unblocking temperatures above the peak metamorphic temperature (and its extension to higher unblocking temperatures predicted by theory as explained above.) Therefore, the magnetization isolated by Weiss et al. (2015) provides no information on the presence or absence of a magnetization that predates the episode of peak metamorphic reheating ($\sim 2650$ Ma).
2. If the Jack Hills sediments have been pervasively remagnetized, the remagnetization direction should be expressed as a single direction (after removal of viscous magnetizations) encompassing low to high unblocking temperatures, as predicted by theory for single domain magnetite grains, and by relaxation of multidomain magnetite grains; the high unblocking temperatures are missing in data presented by Weiss et al. (2015).

As part of our continuing efforts to investigate magnetic particles in the Jack Hills sediments, we present our first results of scanning electron microscope (SEM), energy dispersive X-ray spectroscopy (EDS) and electron microprobe (EMP) analyses, coupled with new paleomagnetic analyses of JH quartzite cobbles. These analyses provide important context for understanding the magnetizations held by zircons (which are not explicitly studied here).

The new analyses confirm the presence of magnetite as an intrinsic detrital oxide phase in Jack Hills quartzite cobbles, including a sample from an outcrop reported in Weiss et al. (2015). Our new paleomagnetic data (and prior analyses reported in Tarduno and Cottrell, 2013), indicate that a ca. 1070 Ma magnetization does not pervasively overprint the sediments of the Jack Hills. We also present new data from an independent laboratory calibration test that verify the unblocking temperature structure and directions reported by Tarduno and Cottrell (2013). Importantly, in these analyses the crucial high unblocking temperature component that Weiss et al. (2015) are unable to isolate is seen. We discuss why some laboratories and their associated experimental protocols cannot define magnetizations on the weakest terrestrial samples that are otherwise within the measurement range of SQUID rock magnetometers. We also provide guidelines (e.g., on appropriate sample sizes, atmosphere for thermal demagnetization, and required magnetometer sensitivity) for other laboratories seeking to investigate such samples with very weak intrinsic magnetizations.

The EMP data define a host of other magnetic oxides that we interpret as the source of a complex series of secondary magnetizations seen at low unblocking temperatures (Tarduno and Cottrell, 2013). We highlight the compositional distinctiveness of magnetic grains, and related non-magnetic sulfides for constraining provenance and addressing the question of whether a Hadean rock fragment is preserved in the Jack Hills sediments (Wilde and Spaggiari, 2007; Tarduno and Cottrell, 2013). A Hadean rock sample could provide insight into the early Earth's physical environment, salient processes, and the origin of life. We suggest that Cr–Fe spinels, Ni-bearing sulfides and some pyrrhotite grains form an assemblage derived from an ultramafic source. The very low Mg content of the spinels leads us to suggest that rather than a komatiitic source, this assemblage reflects erosion of a layered intrusion, fragments of which may be preserved as enclaves in gneiss of the Yilgarn craton. However, any Hadean rock fragment, if present, remains elusive.

## 2. Coupled electron microscopy and paleomagnetic analyses

To examine the magnetic mineralogy of quartzite cobbles from the Jack Hills, we selected several samples from the original collection of Tarduno and Cottrell (2013) for analysis (collected in 2010 and 2011), with new samples collected in 2012. Standard polished 30 μm thin sections were prepared from the interior of the cobbles. During thin section preparation, slides were polished with 1 and 0.3 micron alumina powder. Afterwards, a secondary polishing was done using ∼0.05 micron colloidal silica. These slides were first examined with a Nikon Eclipse LV100POL reflected light microscope at the University of Rochester to identify opaques for SEM study. Following reflected light examination, slides were coated with a ∼15–20 nm thick layer of carbon and analyzed using a Zeiss–Auriga Scanning Electron Microscope at the University of Rochester using secondary and backscattered electron detection modes. Accelerating voltages employed ranged from 5 to 20 kV. Chemical composition of opaques were characterized using energy dispersive X-ray spectroscopy. Electron microprobe analysis was subsequently conducted on opaques characterized by SEM analyses using a Cameca SX-100 at the Rensselaer Polytechnic Institute (RPI). The operating voltage was 15 keV whereas the spot size was ∼500 nm.

Below we discuss illustrative examples of the paleomagnetic behavior linked to the magnetic mineralogy as defined by SEM, EDS and EMP analyses, with an emphasis on the sources of the characteristic remanent magnetization. Because Weiss et al. (2015) emphasize low unblocking temperature components, we select examples which show large low unblocking temperature components. Samples with larger (relative) high unblocking temperature components are discussed in Section 3.

For paleomagnetic measurements, we use a liquid helium 2G Enterprises 3-component DC SQUID (model 755) magnetometer at the University of Rochester with high resolution sensing coils. This instrument is used for measurement of JH cobble samples (as opposed to the 6.3 mm bore ultra-sensitive magnetometer used to measure zircons) because it has a 4.2 cm room-temperature access bore able to accommodate larger samples. These larger samples are in turn needed to ensure that sufficient magnetic material is present in these magnetically weak, bulk sedimentary rocks for reliable measurements. For the measurements discussed in this section, sample volumes are ∼3 cm$^3$, which is a balance between having a sample small enough to avoid secondary features and large enough to contain sufficient magnetic grains. A further discussion of the characteristics of the 755-series SQUID magnetometers and the need to use quartzite sample volumes with enough magnetic grains to yield reliable data is also found in Section 3.

We first discuss cobble JC43 collected in 2012, approximately 300 m along strike (to the NE) from the majority of the 2010 and 2011 samples (Supplementary Figs. S1, S2; GPS coordinates given in Supplementary Table S1). Stepwise thermal demagnetization reveals the removal of low unblocking temperature components of magnetization that do not trend to the origin of orthogonal vector plots, indicating the presence of higher unblocking temperature components (Fig. 1a). We follow the nomenclature of Tarduno and Cottrell (2013) who discussed low unblocking (LT) and intermediate unblocking (IT) temperature components comprising this overall "low" unblocking temperature range. [We note that Weiss et al. (2015) defined LT and "high" unblocking temperature magnetizations, labeling the latter as "HT". We emphasize that there are no coherent high unblocking temperature magnetizations in the data of Weiss et al. (2015). Instead, the "HT" magnetizations of Weiss et al. (2015) were isolated at lower temperatures, corresponding to the unblocking temperatures where the LT and IT magnetizations of Tarduno and Cottrell (2013) were isolated.] The new data from cobble JC43 define both a LT [Inclination (I) = 45.6°, Decli-

nation (D) = 312.5°, maximum angular deviation (MAD) = 6.0°] and an IT (I = −2.3°, D = 114.8°, MAD = 8.0°) component; the former is within 20° of the predicted ca. 1070 Ma field direction [based on paleomagnetic analyses of Wingate et al. (2002), predicted direction of I = 44.9°, D = 339.7°], whereas the latter is far removed from it. Enlargement of the JC43 cobble orthogonal vector plot (Fig. 1b) indicates that the vector does not trend to the origin–defining a characteristic remanent magnetization – until unblocking temperatures higher than 515 °C, exceeding the peak metamorphic temperature. The further demagnetization of the sample indicates unblocking temperatures suggesting a magnetite-like magnetic carrier [HT characteristic remanent magnetizations (ChRM), and LT and IT components are reported in Supplementary Table S2] with a HT ChRM defined between 515 and 545 °C. The magnetization at 545 °C is the last coherent data for this sample; it has an intensity of $5.74 \times 10^{-11}$ A m$^2$ which represents 0.1% of the NRM intensity. SEM, EDS and EMP analyses of JC43 indicate that the opaque assemblage includes magnetite grains (Fig. 1c–h, Supplementary Fig. S3). Some of these grains are sub-rounded, suggesting a detrital origin (Supplementary Fig. S3).

We next discuss cobble JC57 (Fig. 2). This sample was collected off-strike of the 2010–2011 samples, on a bed to the North (Supplementary Fig. S2). Thermal demagnetization data shows some variation, but overall only one dominant direction is suggested from the natural remanent magnetization to treatment at 580 °C, after which the magnetization is essentially at the origin of the orthogonal vector plot (i.e., the fully demagnetized state), with any remaining magnetization attributable to hematite produced from modern weathering. Irrespective of exhaustive attempts to isolate the freshest samples from the interior of the cobbles, Tarduno and Cottrell (2013) emphasized the ubiquity of hematite linked to modern weathering. The demagnetization data, however, are too linear from low to high unblocking temperatures for the preservation of an ancient magnetization (especially in light of the metamorphic history since deposition) and we attribute the magnetization of this sample to reflect a modern lightning strike. Note that the magnetic remanence also extends in a linear fashion between 500 and 580 °C (Fig. 2b), indicative of a magnetite magnetic carrier. Although demagnetized to 1.3% of the NRM, the intensity at 580 °C ($1.03 \times 10^{-8}$ A m$^2$) is unusually strong, consistent with a lightning strike magnetization. SEM, EDS and EMP analyses confirm the presence of sub-rounded magnetite in this clast as an original part of the opaque assemblage (Fig. 2c–h; Supplementary Fig. S4). The location of this cobble overlaps with those reported by Weiss et al. (2015) (Supplementary Fig. S2), and appears to be from the same outcrop. Weiss et al. (2015) also interpret samples from this outcrop as having been hit by lightning. The direction isolated from cobble JC57 differs from those reported by Weiss et al. (2015) but some declination values are similar; a large variation in magnetic direction over small distances, however, is common in outcrops struck by lightning. An unexpected difference, however, is the lack of any coherent magnetic direction at unblocking temperatures >400 °C in the data of Weiss et al. (2015). After treatment at this temperature, the magnetization of the Weiss et al. (2015) samples are in the $10^{-9}$ to $10^{-10}$ A m$^2$ range, intensities that are typically measurable with modern SQUID rock magnetometers.

We next discuss cobble JC64, collected in 2012, located at the far southwestern end of the cobble bed collected in 2010–2011 (Supplementary Fig. S2). Thermal demagnetization of this sample also reveals the removal of a large component of natural remanent magnetization at unblocking temperatures less than 350 °C, defining a direction that does not trend to the origin of the orthogonal vector plot (Fig. 3a). Here we define LT and IT components between 250 and 300 °C, and 375 and 425 °C, respectively (Supplementary Table S2). Enlargement of the plot again shows that
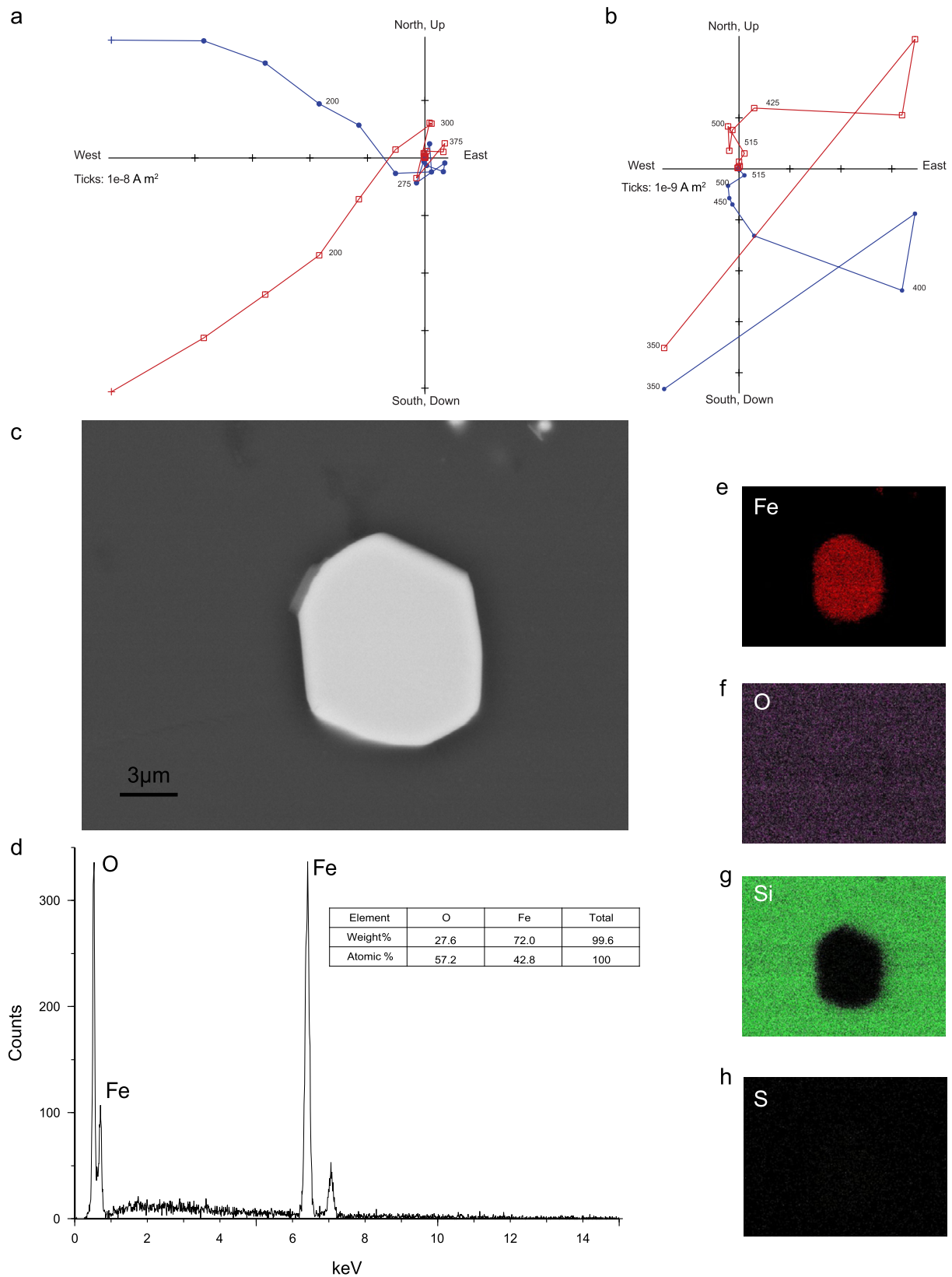
**Fig. 1.** Results for cobble JC43. a. Orthogonal vector plot of stepwise thermal demagnetization. Labeled steps are °C. b. Enlargement of (a), showing high unblocking temperature steps. c. Scanning electron microscope image (backscatter detector) of oxide grain which is iron rich in energy dispersive spectroscopy (d) and with weight and atomic percentages from electron microprobe (EMP) analyses indicating a magnetite composition. EMP standards for this and other analyses presented here are as follows: magnetite, Minas Gerais, Brazil, Smithsonian USNM #114887; hematite, locality unknown (RPI); troilite, Staunton, VA., American Museum of Natural History; pyrite, locality unknown (RPI); orthoclase, OR-1, synthetic, Harvard/Geophysical Lab, Carnegie Institution; rutile, Manford Co. MD, Harvard #323; chromite, New Caledonia, Smithsonian USNM #117075; nickel, locality unknown (RPI); diopside, Di2Ti synthetic, Geophysical Lab, Carnegie Institution; jadeite, Santa Rita Peak, San Benito Co. CA, Harvard #184; kyanite, Synthetic, Bell Laboratories; forsterite, SynForsterite synthetic, Harvard #84; cerium phosphate, $CePO_4$, synthetic (RPI), zinc, synthetic zinc oxide, produced by John Ferry (Johns Hopkins University). (e–h) Maps of Fe, O, Si and S (K shell).
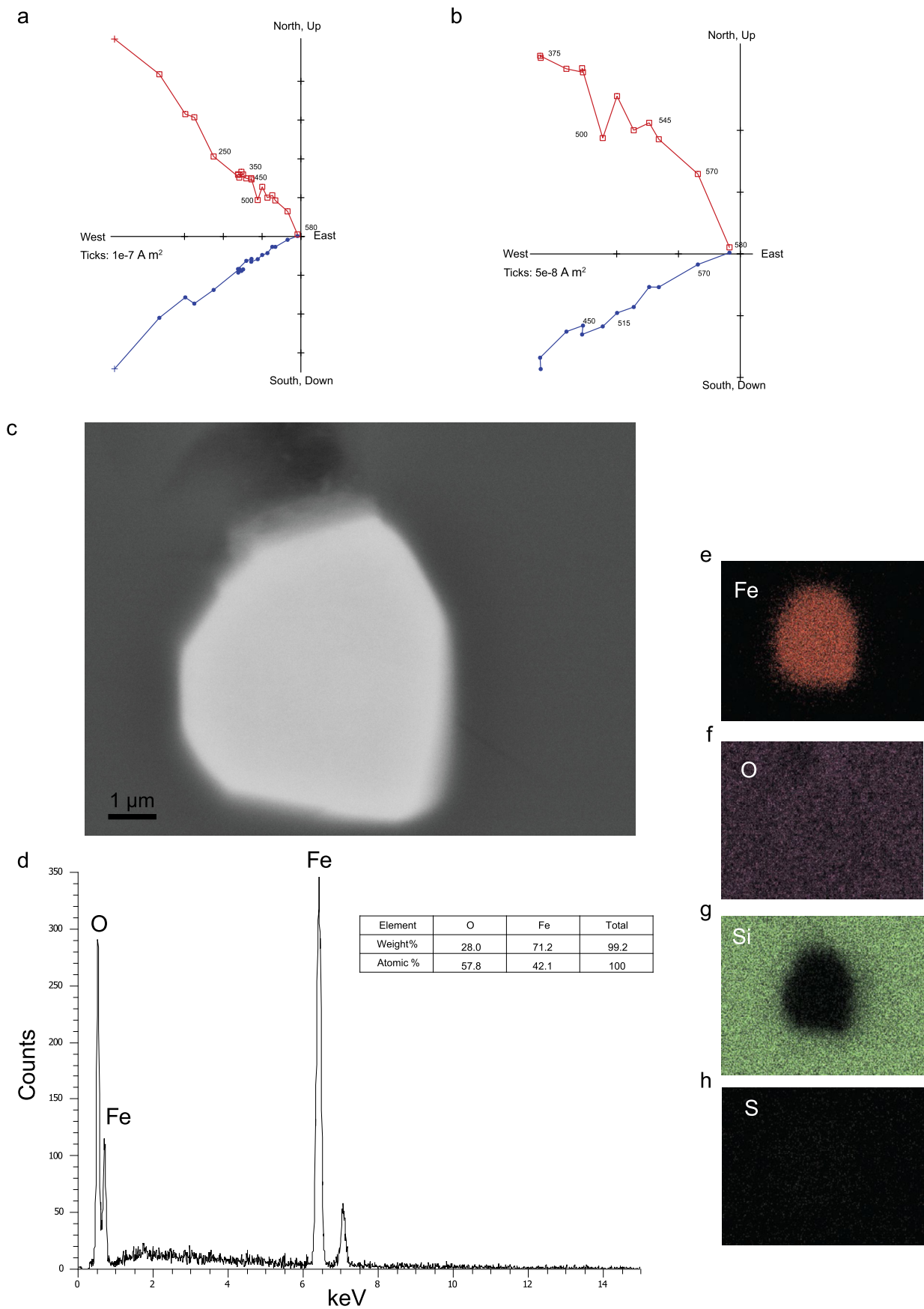
**Fig. 2.** Results for cobble JC57. a. Orthogonal vector plot of stepwise thermal demagnetization. Labeled steps are °C. b. Enlargement of (a), showing high unblocking temperature steps. c. Scanning electron microscope image (backscatter detector) of oxide grain which is iron rich in energy dispersive spectroscopy (d) and with weight and atomic percentages from electron microprobe analyses indicating a magnetite composition. (e–h) Maps of Fe, O, Si and S (K shell).

the vector does not trend to the origin until high unblocking temperatures (Fig. 3b). A HT ChRM is defined at temperatures between 545 and 580 °C, corresponding to intensities of $5.94 \times 10^{-11}$ Am$^2$ and $1.18 \times 10^{-11}$ Am$^2$, respectively (both <1% of the NRM). None of the directions from cobble JC64 corresponds to the ca. 1070 Ma predicted direction. SEM and EDS analyses suggest the presence of weathered and/or altered magnetite grains as part of the *in situ* opaque assemblage (Figs. 3c–h). EMP analyses suggest that the grains have undergone various levels of transformation to maghemite or hematite, showing reaction rims and/or transformation along cracks (Supplementary Fig. S5).

We next consider cobble JC30, collected in 2012, at the far northeast exposure of the cobble beds sampled (Supplementary Fig. S2). A LT component is present (Supplementary Table S2); this direction is far removed from the ca. 1070 Ma predicted direction. A cursory examination of these data (Fig. 4a) could lead to a misinterpretation: complete demagnetization by 300 °C. Enlargement of the orthogonal vector plot, however, shows that the vector does not trend to the origin until temperatures exceeding the peak metamorphic temperature (Fig. 4b). However, at temperatures >515 °C (where the intensity is $9.87 \times 10^{-11}$ Am$^2$ and 1% of the NRM) directions vary too greatly to define a direction with a reasonable confidence interval (although the data clearly indicate that a HT component is present). SEM, EDS and EMP analyses indicate the presence of altered magnetite grains as part of the *in situ* opaque assemblage (Fig. 4c–h). These include grains with shrinkage cracks that are the signature of maghemitization. Also included in this cobble are rare Ti–Fe oxides possibly showing exsolution features (Supplementary Fig. S6); these may be in part titanohematite (Lagroix et al., 2004; Burton et al., 2008) that was suggested in some low temperature magnetic susceptibility data (Tarduno and Cottrell, 2013). The latter [Fig. 3A, D, and E of Tarduno and Cottrell, 2013] suggested Curie temperatures below room temperature.

Tarduno and Cottrell (2013) predicted the presence of pyrite in some samples that upon laboratory heating transformed to pyrrhotite (e.g. Li and Zhang, 2005; Chou et al., 2012). Pyrite is also seen as an opaque mineral in some samples (Fig. 5, Supplementary Fig. S7), including rounded and pyritohedron forms (pentagonal dodecahedron), confirming the prediction derived from magnetic susceptibility data.

Other sulfides found in some cobble samples include pyrrhotite [Fe$_{1-x}$ ($x$ = 0 to 0.17)] (Fig. 6, Supplementary Fig. S8), pentlandite [(Fe,Ni)$_9$S$_8$] (Supplementary Fig. S9) and rare smythite [(Fe,Ni)$_9$S$_{11}$ or (Fe,Ni)$_{13}$S$_{16}$] (Supplementary Fig. S10). The Ni-bearing phase pentlandite is non-magnetic. The occurrence of pyrrhotite is not surprising within the context of the other opaque minerals, however the absence of a clear indication of the characteristic Curie temperature of 325 °C in magnetic susceptibility data versus temperature data (Tarduno and Cottrell, 2013) suggests that rather than the monoclinic phase, these pyrrhotites are predominantly hexagonal (e.g. Fe$_9$S$_{10}$ and Fe$_{11}$S$_{12}$). The associated Curie temperatures of hexagonal pyrrhotite (or more correctly the stability range of λ-pyrrhotite) range between 210 and ~265 °C (Schwarz and Vaughan, 1972), and this range might account for the absence of a clear signal in the magnetic susceptibility versus temperature data. However, the overall magnetic susceptibility signal appears to be dominated by magnetite and oxidized magnetite grains. Because hexagonal pyrrhotite is only ferrimagnetic between its λ transition at ~200 °C and the upper temperature range of its stability, it is not expected to carry remanence of geologic significance (Dunlop and Özdemir, 1997). EMP data (Fig. 6, Supplementary Fig. S8 and Supplementary Tables S3, S4) confirm the dominance of hexagonal pyrrhotite in the cobbles analyzed. We also emphasize that while pyrrhotite commonly occurs as a late chemical alteration phase in younger sedimentary rocks, the pyrrhotite in these samples ap-

pears to be detrital. The co-occurrence of detrital pyrite argues against pyrrhotite formation (from pyrite) during metamorphism of the JH sediments.

Finally, we note the presence of Cr–Fe spinels (Fig. 7, Supplementary Fig. S11). This occurrence is not surprising given that fuchsite is commonly seen in the JH sediments, but nonetheless it is important as an indicator of an ultramafic source quite different from the granitoid source of the zircons. The Cr–Fe spinels have a range of Curie temperatures (Robbins et al., 1971), but altered phases typically have Curie temperatures in the range of 120–450 °C (Kadziałko-Hofmokl et al., 2008).

More specifically, Curie temperatures decrease as the mole fraction of Cr$^{+3}$ ($n$) increases. Solid solutions having $n \geq 0.6$ are ferromagnetic below room temperature. It is possible to estimate Curie temperature given $n$ (Robbins et al., 1971; Ziemniak and Castelli, 2003). Cations of Al, Mg, Mn, Ni and Ti may also influence the magnetic properties of Fe–Cr spinels. It is the ratio of Cr to cations within the B sublattice of the spinel structure that are of interest. On the basis of our EMP data, estimates of $n$ range from ~0.35 to 0.5, suggesting Curie temperatures between ~300 to ~120 °C, respectively. Samples with comparatively higher weight percent of Fe and lower weight percent of Cr (Supplementary Fig. S11) would represent higher Curie temperatures. High Fe phases of Fe-Cr spinel in our samples tend to be less pristine, as observed in SEM images.

The JH cobble samples thus show a large range of opaque mineralogies. The list of opaque minerals that can contribute to the low unblocking temperatures includes coarse magnetite and maghemite, monoclinic pyrrhotite, and Cr–Fe spinels. As opposed to many younger settings where sulfide minerals are predominately associated with late fluids and are often found along fractures, sulfides in our JH cobble samples occur as isolated grains in the quartzite and appear to be predominantly detrital (note rounded grains, e.g., Figs. 5–6, Supplementary Figs. S7A and S8A). The presence of pigmentary hematite can also contribute to low unblocking temperatures magnetizations (e.g. Tarduno et al., 1992). Importantly, magnetite crystals, appearing as angular to sub-rounded grains, are present as parts of the *in situ* opaque mineral assemblage. Thus, the prediction that magnetite is present, as previously indicated by the magnetic susceptibility versus temperature data of Tarduno and Cottrell (2013) that document a Verwey transition, and the high unblocking temperatures (~550–580 °C) reported by Tarduno and Cottrell (2013), is confirmed. This highlights the question of why Weiss et al. (2015) were unable to isolate a high unblocking temperature magnetization carried by magnetite. Below, we examine this through a comparison study with a third laboratory, which also serves to document the procedures and magnetometer sensitivity needed to accurately record the JH sediment magnetizations. We return to the important question of what information the diverse detrital mineralalogies we have documented can place on JH sediment provenance in Section 4.

## 3. Inter-laboratory test data

Samples from the Tarduno and Cottrell (2013) study were measured using the same liquid helium 2G 3-component DC SQUID (model 755) magnetometer at the University of Rochester as employed here. The use of 3-component systems is important when trying to resolve weak multi-component magnetizations because they do not have the inherent problems of non-uniqueness associated with use of 1-component systems (such as scanning SQUID microscopes) when measurement noise is non-negligible [e.g., Parker, 1991]. The pickup coil diameter and spacing of the 2G 3-component systems merits some additional explanation.
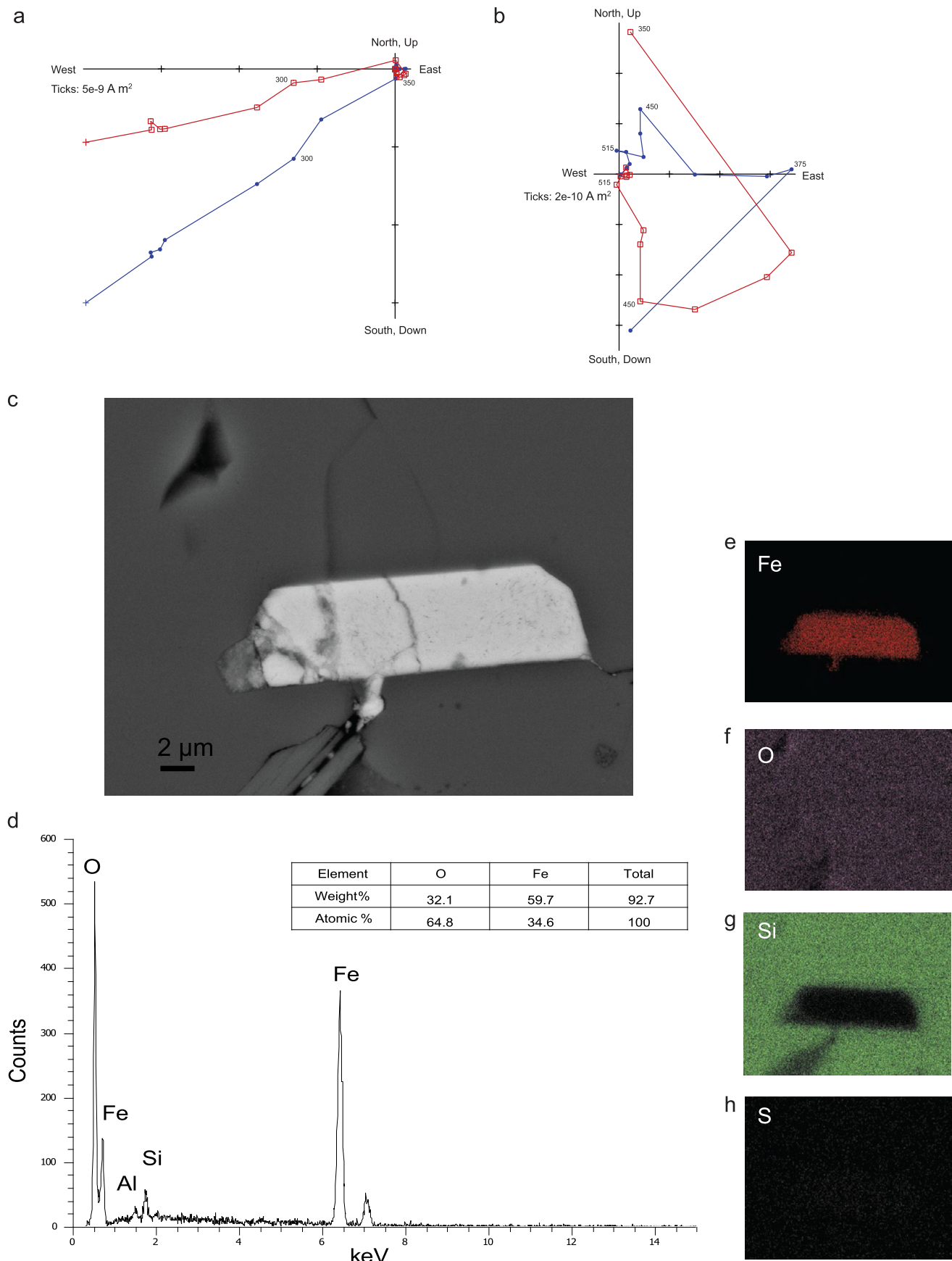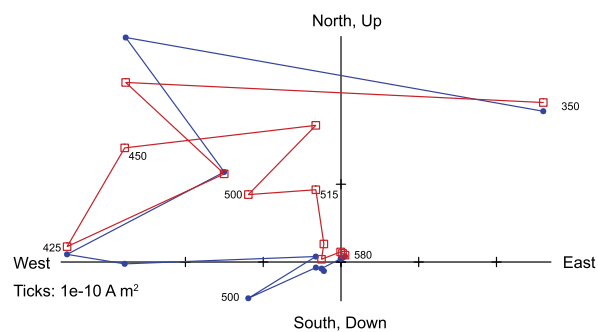
**Fig. 3.** Results for cobble JC64. a. Orthogonal vector plot of stepwise thermal demagnetization. Labeled steps are °C. b. Enlargement of (a), showing high unblocking temperature steps. c. Scanning electron microscope image (backscatter detector) of oxide grain which is iron rich in energy dispersive spectroscopy (d) and with weight and atomic percentages from electron microprobe analyses indicating an oxidized magnetite (maghemite) composition. (e–h) Maps of Fe, O, Si and S (K shell).
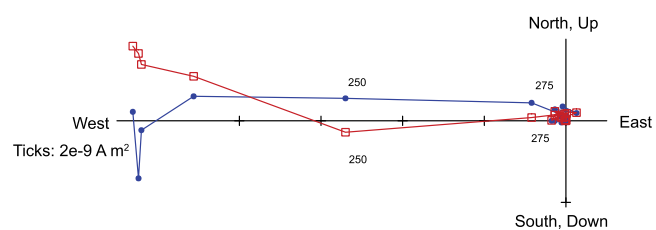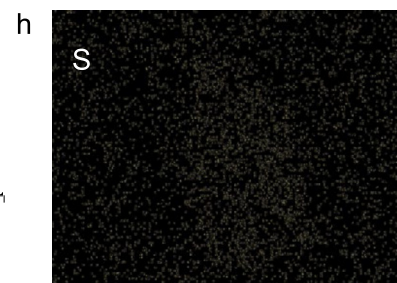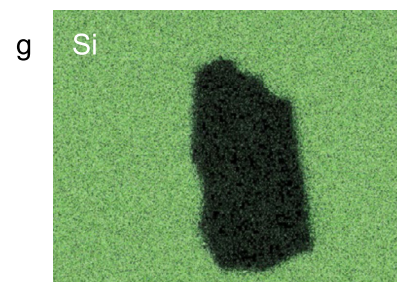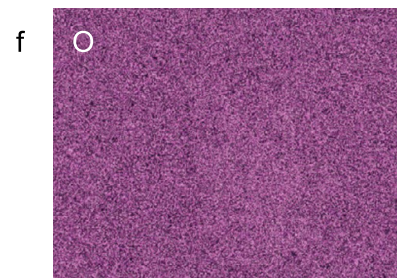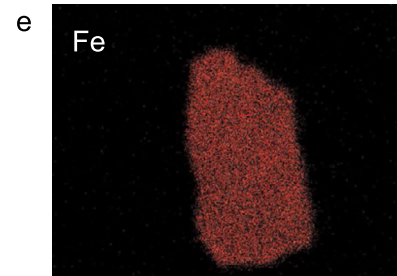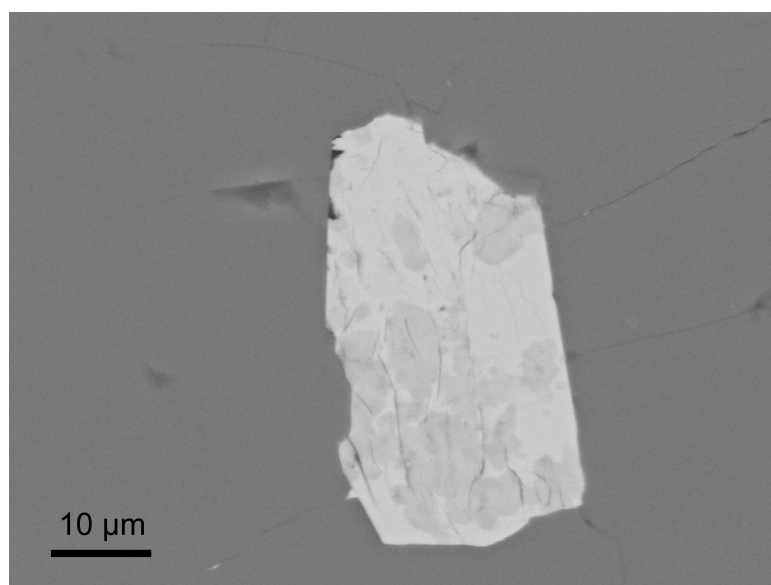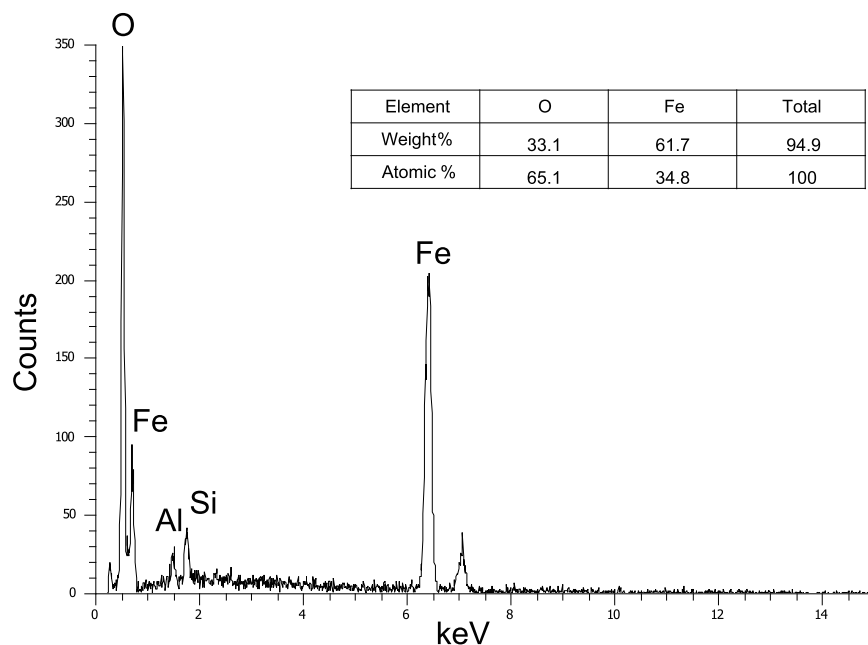
**Fig. 4.** Results for cobble JC30. a. Orthogonal vector plot of stepwise thermal demagnetization. Labeled steps are °C. b. Enlargement of (a), showing high unblocking temperature steps. c. Scanning electron microscope image (backscatter detector) of oxide grain which is iron rich in energy dispersive spectroscopy (d) and with weight and atomic percentages from electron microprobe analyses indicating an oxidized magnetite (maghemite) composition. (e–h) Maps of Fe, O, Si and S (K shell).

a



b



| Element | S | Fe | Total |
|---------|------|------|-------|
| Weight% | 54.0 | 46.3 | 101 |
| Atomic % | 66.8 | 32.9 | 100 |

c



Fe

d



O

e



Si

f



S
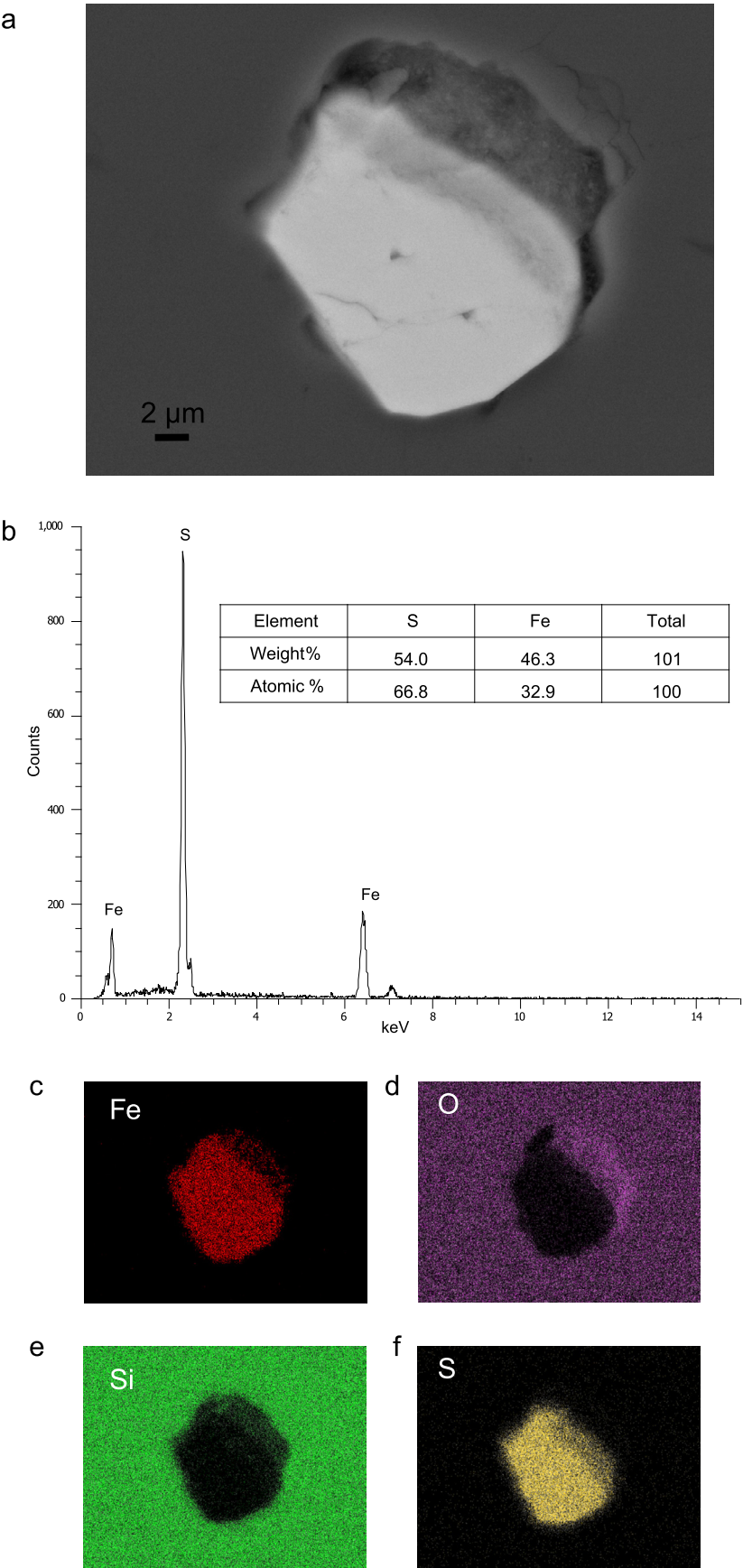
**Fig. 5.** Results for cobble JC64 showing pyrite grain. a. Scanning electron microscope image (backscatter detector) (b) EDS, weight and atomic percentages from electron microprobe analyses (inset). (c–f) Maps of Fe, O, Si and S (K shell).

| Element | S | Fe | Total |
|---------|------|------|-------|
| Weight% | 37.7 | 59.9 | 98.2 |
| Atomic % | 51.6 | 47.1 | 100 |
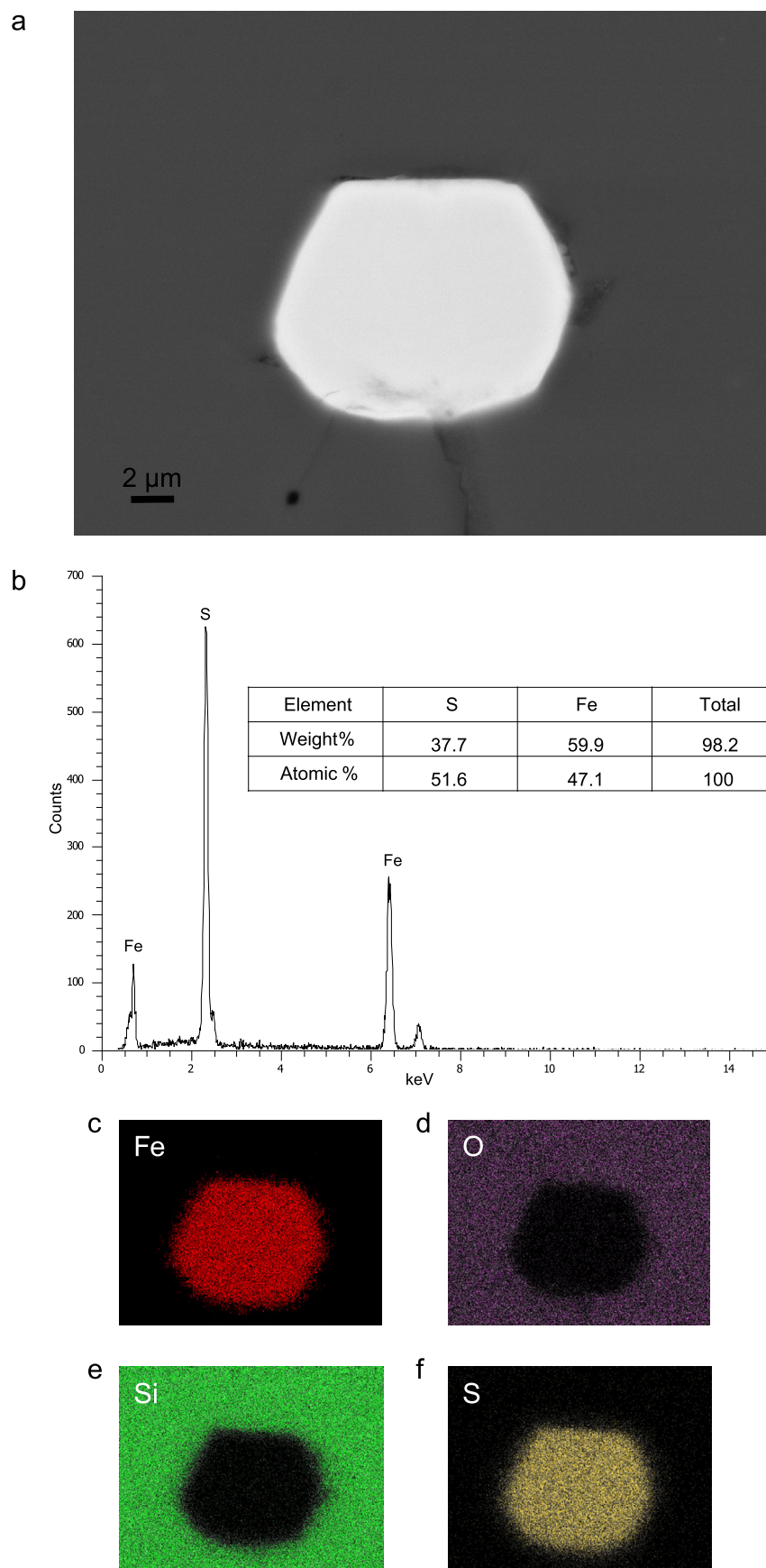
**Fig. 6.** Example of pyrrhotite particle from cobble JC43. a. Scanning electron microscope image (backscatter detector) (b) EDS, weight and atomic percentages from electron microprobe analyses (inset). (c–f) Maps of Fe, O, Si and S (K shell).

a



20 µm

b

| Element | Ca | Ti | Fe | Cr | Ni | Al | Mg | Mn | O | Total |
|---|---|---|---|---|---|---|---|---|---|---|
| Weight % | -0.01 | 0.29 | 25.6 | 36.2 | -0.01 | 5.82 | 0.23 | -0.02 | 33.2 | 101 |
| Atomic% | -0.01 | 0.18 | 13.2 | 20.1 | -0.01 | 6.23 | 0.27 | -0.01 | 60.0 | 100 |



c Fe    d O

e Si    f Cr
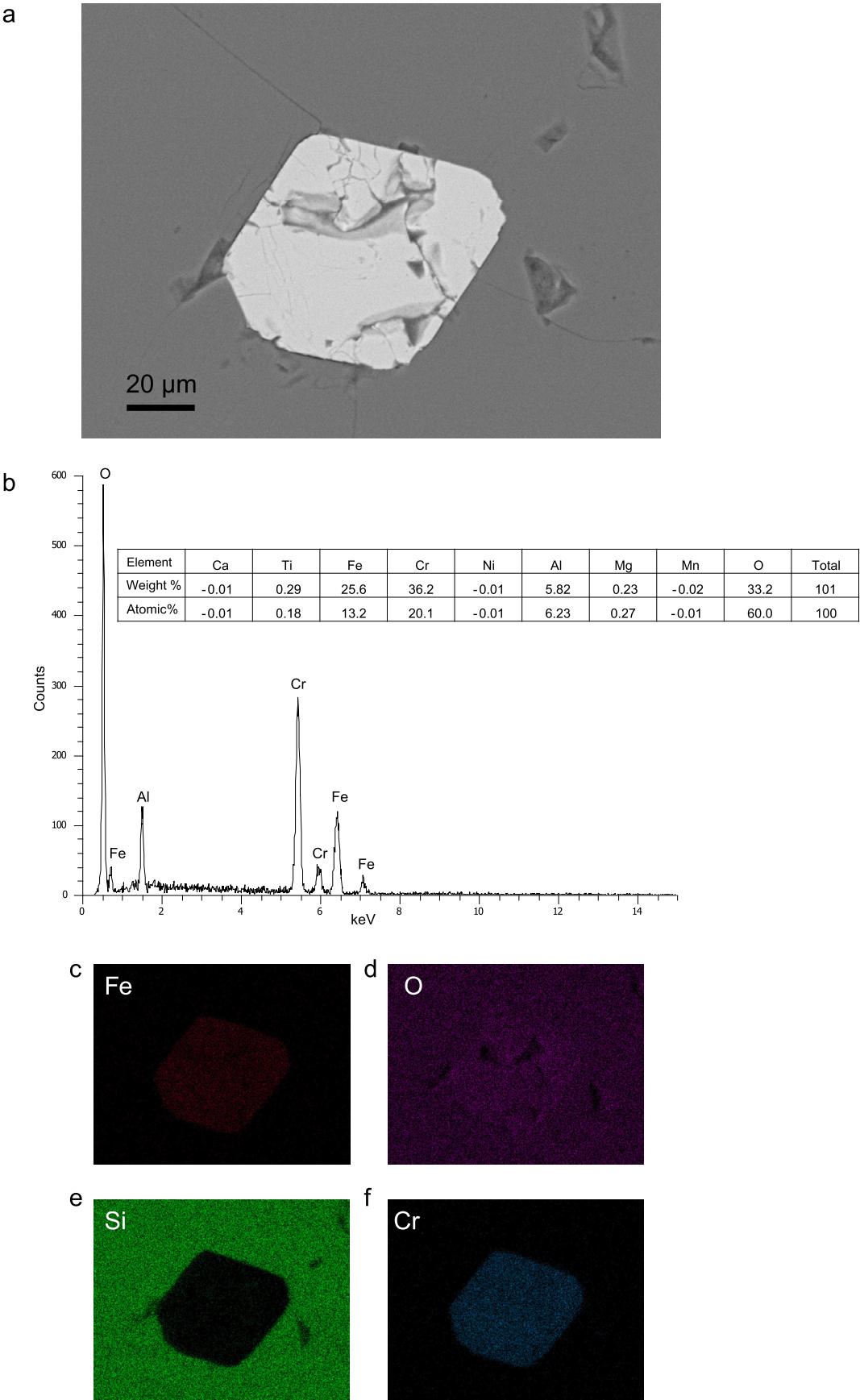
**Fig. 7.** Example of Cr–Fe-spinel from cobble JC64. a. Scanning electron microscope image (backscatter detector) (b) EDS, weight and atomic percentages from electron microprobe analyses (inset). (c–f) Maps of Fe, O, Si and Cr (K shell).

A smaller room temperature access bore allows a smaller coil diameter and higher sensitivity. Thus, a "standard" model 755 geared toward high resolution has a 4.2 cm bore. Instruments with larger bores to incorporate large samples have also been manufactured by 2G Enterprises. Most standard model 755's have a pickup coil spacing that is commonly called a "high homogeneity" geometry because it provides a relatively large sensing region. Higher sensitivity can be reached using a smaller coil spacing; this is called a "high resolution" coil geometry. The University of Rochester 755 magnetometer has the high resolution spacing. In this case, samples must be positioned exactly in the center of the coils. For University of Rochester measurements, an eight-position sampling routine is used; this routine also provides internal averaging. For the Tarduno and Cottrell (2013) study, an ultra-low mass sample holder was used with negligible moment ($< 1 \times 10^{-12}$ A m$^2$). For those outside the discipline of paleomagnetism, it is important to note that not all 2G SQUID magnetometers of the same model have the same noise levels, and external factors (e.g., building housing the magnetometer and setting) also play important roles. The practical background level of the University of Rochester system of $9 \times 10^{-13}$ A m$^2$ is viewed as exceptional for magnetometers of this generation.

We initially entered into collaboration with the Weiss et al. (2015) group. We provided unpublished information on field localities, sample types, sample preparation, intensities, demagnetization parameters, rock magnetism, and magnetic mineralogy. We offered measurements, but received no suitable samples (Supplementary Fig. S12). Therefore, we sought collaboration from a third lab.

For comparison, we use a 2G 3-component DC SQUID (model 755) magnetometer at Lehigh University (4.2 cm bore). This magnetometer has high homogeneity coils and therefore is less sensitive than the Rochester 755 magnetometer, but external factors (building and campus) are roughly comparable [in contrast, the housing of the magnetometer used by Weiss et al. (2015) is unusual; it is located high in a tall, narrow building (MIT Building 54)]. In addition, the Lehigh University system utilizes a custom made Delrin sample holder for single specimen measurements with a relatively high mass and associated moment ($\sim 3 \times 10^{-11}$ A m$^2$), which is ultimately an important limitation in reaching the lowest sensitivities potentially available.

We selected 4 samples from the cobble sample suite reported in Tarduno and Cottrell (2013) with the following caveats: *i.* samples toward the larger range of initial natural remanent magnetizations were selected to ensure that they would be within the measurement range of the Lehigh magnetometer given the practical considerations discussed above, *ii.* the volumes of samples were approximately a factor of 2 greater for the Lehigh measurements than those used in the Rochester study and *iii.* the optimal subsample for the interior of any given cobble (i.e., that subsample having the least amounts of secondary features such as veins and secondary staining due to pigmentary hematite) had already been measured in the prior study, so a slightly less desirable (but still acceptable) subsample had to be chosen. This could be done for three of the cobbles, but for the fourth (sample JC16) pigmentary hematite staining could not be avoided. We discuss the specific results in detail below.

### 3.1. JC15

The characteristic remanent magnetization results from JC15 are most similar between the two laboratories (Fig. 8); the natural remanent magnetization of the Lehigh University sample is 6.8 times greater than the University of Rochester sample, which is greater than the difference attributable to volumes (factor of $\sim 2.1$), and must reflect some difference in bulk magnetic mineral con-

tent. The Lehigh University subsample has a greater proportion of natural remanent magnetization removed at low unblocking temperatures. While the Lehigh data is more scattered at the high unblocking temperatures, the direction isolated between 510 and 560 °C (I = 24.1°, D = 150.4°, MAD = 25.9°, intensities ranging from $2.23 \times 10^{-9}$ to $1.73 \times 10^{-9}$ A m$^2$) is similar to the results from the University of Rochester sub-sample isolated at temperatures between 560 and 580 °C (I = 6.7°, D = 137.6°, MAD = 2.1°, intensities ranging from $5.31 \times 10^{-9}$ to $8.68 \times 10^{-11}$ A m$^2$) (Fig. 8). More conservatively, the Lehigh University data clearly indicate the presence of a high unblocking temperature magnetization.

### 3.2. JC1

Results from both the Lehigh and Rochester labs indicate the presence of a high unblocking temperature component in samples from cobble JC1 (Fig. 9), but with differences in the resolution of the vector at the high unblocking temperatures. Natural remanent magnetization values between samples vary by a factor of $\sim 4.9$, similar to that predicted by the volume difference ($\sim 4.4$). At unblocking temperatures greater than approximately 400 °C, the Lehigh University data when viewed on an orthogonal vector plot (Fig. 9) crosses the N–S axis whereas the Rochester data remain in the N–W quadrant. However, the subtracted vector in the Lehigh data between 540 and 560 °C (I = 68.3°, D = 339.3°, MAD = 23.9°, intensities ranging from $2.88 \times 10^{-10}$ to $2.15 \times 10^{-10}$ A m$^2$) and the Rochester data isolated between 560 and 580 °C (I = 42.2°, D = 343.5°, MAD = 8.2°, intensities ranging from $3.84 \times 10^{-11}$ to $2.89 \times 10^{-11}$ A m$^2$) are similar. We interpret the difference in the data to mainly reflect the greater influence of hematite in the Lehigh sample that displaces the slightly lower blocking magnetite component away from the origin of the orthogonal vector plot.

### 3.3. JC10

The NRM difference between the Lehigh and Rochester samples (a factor of $\sim 3.1$) is greater than the volume difference ($\sim 2.1$) (Supplementary Fig. S13). There is a greater range of remanence at higher unblocking temperatures in the Rochester sample than the Lehigh sample; the more rapid decrease in intensity in the Lehigh sample, however, more quickly results in remanence values close to measurement sensitivity limits, resulting in scattered results at high unblocking temperatures.

### 3.4. JC16

The difference in NRM intensities ($\sim 3.4$ times) is slightly higher than expected for the volume difference (a factor $\sim 1.9$) (Supplementary Fig. S14). The Lehigh University sample has not demagnetized by treatment to 600 °C (after which the demagnetization experiment was halted) clearly indicating a hematite component that is not dominant in the Rochester sample. We conclude the high unblocking temperature magnetite component cannot be retrieved from this sample due to the presence of hematite (as anticipated by the red pigment relative to the University of Rochester sample).

The results from the Lehigh University paleomagnetism laboratory approximate those from the University of Rochester lab, even though the practical background levels of the Lehigh SQUID magnetometer are much higher. As expected, there is more scatter exhibited at the low intensity levels as measured in the Lehigh system, when sample magnetization values reach the practical sensitivity limit at high unblocking temperatures. This, together with the presence of hematite accounts for differences in the two data sets. Specifically, for two of the pairs where the Lehigh and
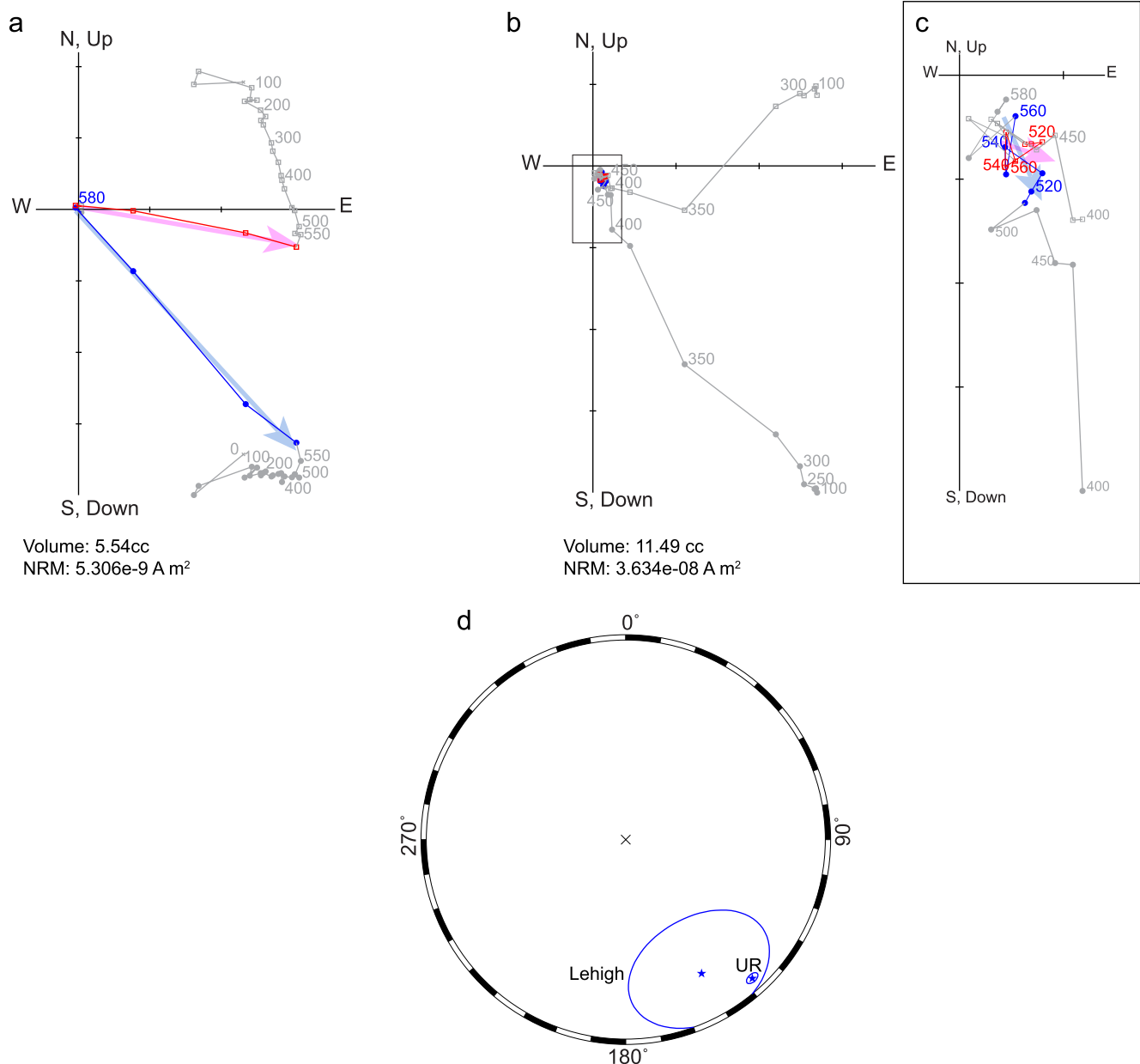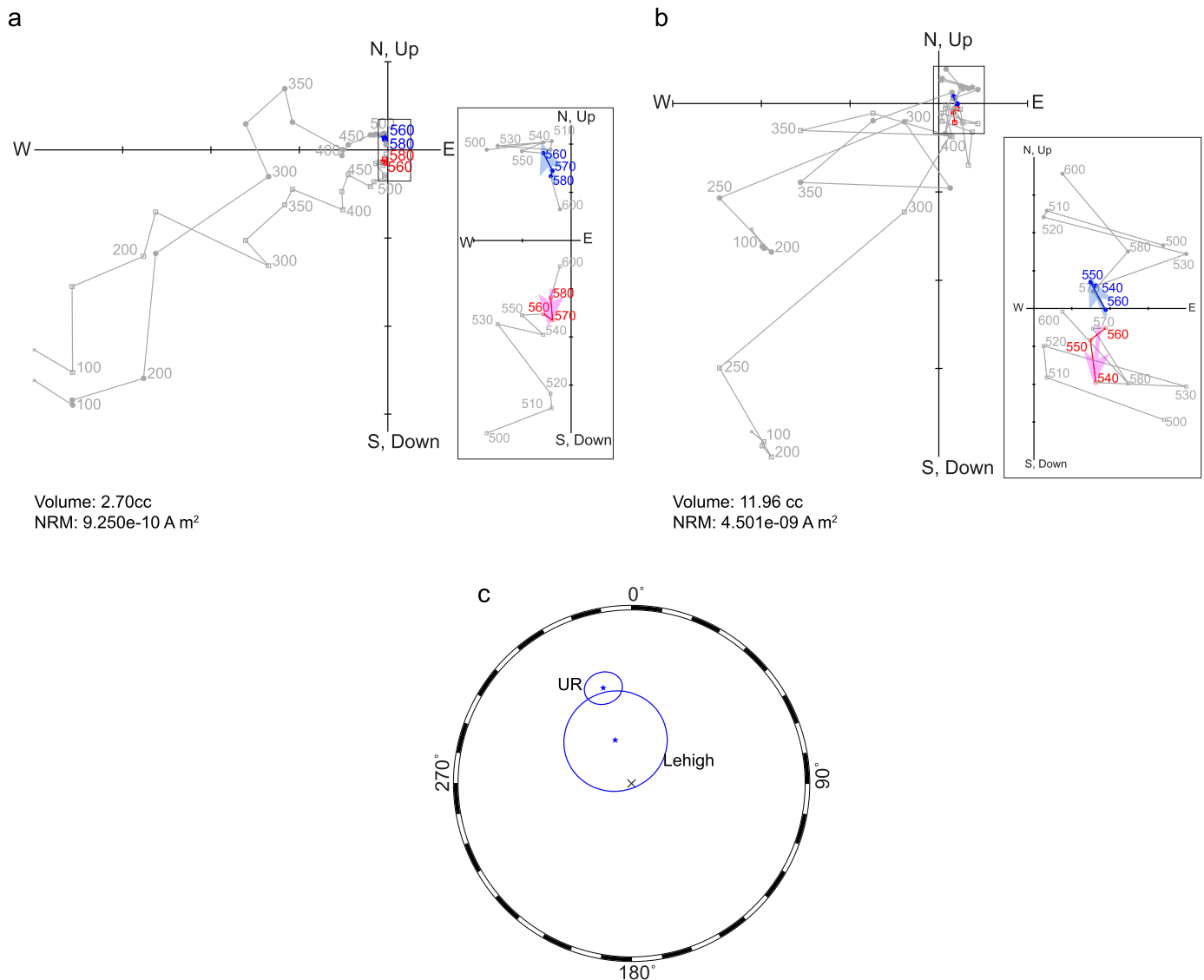
**Fig. 8.** Orthogonal vector plots of thermal demagnetization data from cobble JC15 as measured by two paleomagnetic labs. Horizontal (declination) projection shown by closed circles; vertical (inclination) projection shown by open squares. Highlighted in color is the characteristic remanent magnetization component (red, inclination; blue, declination). (a) Demagnetization of cube cut from the center of cobble, measured at the University of Rochester (UR) from Tarduno and Cottrell (2013). (b) Demagnetization of an additional cube cut from the center of the cobbles, measured at Lehigh University. Box near the origin of the orthogonal vector plot represents enlargement of dataset at higher temperatures (c). (d) Stereographic projection of fit directions.

Rochester samples are most similar in terms of avoiding pigmentary hematite (JC15 and JC1) we see agreement in the isolated characteristic remanent magnetization at high unblocking temperatures, although as expected the Lehigh data have more scatter at the highest demagnetization levels. For JC10, the higher background Lehigh University system prevent resolution of the highest unblocking magnetizations, whereas hematite in the subsample of JC16 similarly prevents the clear definition of a high unblocking temperature magnetization. Although not a focus of this comparison, the low unblocking temperature magnetization results show some similarities between laboratories, but also larger differences, which probably reflect variation in the content of large magnetic grains with short relaxation times between samples.

We also note that for 3 of the 4 test samples, NRM intensity does not scale linearly with volume. The probability of a sample containing horizons with relatively high magnetic mineral contents appears to increase with volume, as expected in the quartzite lithology. Conversely, very small samples might not contain enough magnetic minerals to record magnetizations above magnetometer background levels (see further discussion below).

Importantly, the demagnetization data indicate that significant components of magnetization persist above the temperature of peak metamorphism. This is expressed in two ways: *i.* The final or characteristic magnetization should trend to the origin when viewed on an orthogonal vector plots; if it does not, an unresolved component is present. The directions at unblocking temperatures below ∼500 °C do not trend to the origin of orthogonal vector plots indicating the presence of another component and *ii.* In some cases the high unblocking temperature can be resolved by its trend to the origin.

**Fig. 9.** Orthogonal vector plots of thermal demagnetization data from cobble JC1 as measured by two paleomagnetic labs. Horizontal (declination) projection shown by closed circles; vertical (inclination) projection shown by open squares. Highlighted in color is the characteristic remanent magnetization component (red, inclination; blue, declination). (a) Demagnetization of cube cut from the center of cobble, measured at the University of Rochester (UR) from Tarduno and Cottrell (2013). Box near the origin of the orthogonal vector plot represents enlargement of dataset at higher temperatures. (b) Demagnetization of an additional cube cut from the center of the cobbles, measured at Lehigh University. Box near the origin of the orthogonal vector plot represents enlargement of dataset at higher temperatures. (c) Stereographic projection of fit directions.

In contrast, all data reported by Weiss et al. (2015) on cobbles and other JH sediments are dominated by noise at high unblocking temperatures (although some of the MIT data do not trend toward the origin of orthogonal vector plots indicating an unresolved high unblocking temperature component). Specifically, we see little or no evidence for coherent directions in the Weiss et al. (2015) data at intensities in the $10^{-10}$ A m$^2$ range (magnetizations clearly recorded by the Lehigh and Rochester laboratories). Sources for noise which can mask high unblocking temperature magnetizations in sediments carrying weak magnetizations are considered below.

## 4. Discussion

### 4.1. Detrital magnetite and remanence

In mature sediments like those of the Jack Hills (Eriksson and Wilde, 2010), magnetite is an expected part of the detrital mineral assemblage. The presence of magnetite is important because it has high unblocking temperatures that can potentially see through the peak metamorphic temperatures that the JH sediments have experienced. Our SEM, EDS and EMP analyses confirm that magnetite is present in the JH cobble quartzite samples, as predicted by previous magnetic measurements (Tarduno and Cottrell, 2013). The sizes identified under electron microscopy suggest a multidomain or pseudosingle domain state. But these particles likely reflect the tail at large grain sizes of a distribution that contains smaller single domain grains [as supported by the distribution of magnetic hysteresis values which show evidence of the mixing of large to small grain sizes, cf. Fig. 2 of Tarduno and Cottrell, 2013] which will dominate the high unblocking temperature magnetization.

The samples reported by Weiss et al. (2015) appear to be from a different stratigraphic horizon from those of Tarduno and Cottrell (2013), but the continued sampling of our group removes this ambiguity; our samples from the same outcrop sampled by Weiss et al. (2015) clearly contain primary (detrital) magnetite (Fig. 2, Supplementary Fig. S4). Below we outline four likely reasons why Weiss et al. (2015) were unable to isolate the key high unblocking temperature magnetic component carried by the Jack Hills sediments. These aspects are not mutually exclusive; they provide
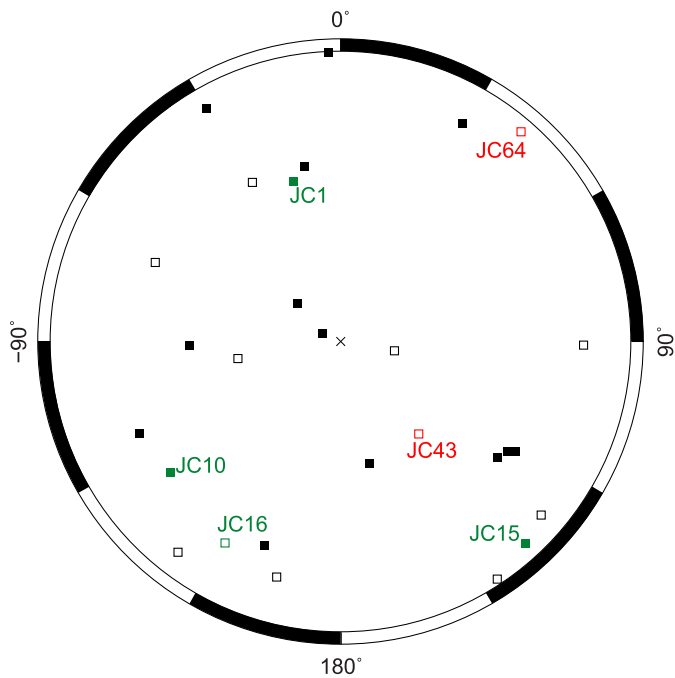
**Fig. 10.** Stereonet of characteristic remanent magnetizations from high unblocking temperature components from thermal demagnetization data (after Tarduno and Cottrell, 2013). Open symbols are negative inclination, closed positive inclination. Highlighted are data that represent the focus of this study. Green squares, from Tarduno and Cottrell (2013). Red squares, this study.

some useful guidelines for those wishing to conduct studies of similar weak sedimentary rocks.

*1. Atmosphere during thermal demagnetization.* It is of utmost importance to match the atmosphere (oxygen fugacity) during thermal demagnetization with the magnetic characteristics of a sample. For example, Ar is often used in the demagnetization of terrestrial and extraterrestrial rocks (e.g. some terrestrial basalts) with favorable results. In contrast, thermal treatment in Ar in highly oxidized materials can severely compromise paleomagnetic data: oxygen is quickly consumed through further oxidation of minerals and a reducing environment can form inside samples. In particular, pigmentary hematites with their large surface areas may be reduced to magnetite. Because samples are heated in field free space, directional data can still be preserved during the initial phases of this magnetite production. In practice, however, soon after the reduction begins, samples acquire stray magnetizations rendering magnetic directional data at high unblocking temperatures highly scattered and unreliable for paleomagnetic analysis. Although care was taken to limit the select samples with a minimum of modern day weathering, the influence of this in the Jack Hills sediments is ubiquitous. As a result, Tarduno and Cottrell (2013) elected to demagnetize samples in air rather than Ar to avoid the problems associated with sample reduction and magnetite formation. This contrasts with Weiss et al. (2015) who used an Ar atmosphere (B. Weiss, personal communication, 2014). The deleterious effects of sequential heating in Ar (vs. Air) are also demonstrated in magnetic susceptibility data [cf. Fig. 3D–E of Weiss et al., 2015]. Therefore, the high unblocking temperature remanence data from Weiss et al. (2015) are probably compromised by laboratory induced reduction of their samples.

*2. Sample size.* For the measurement of extremely weak sedimentary samples, it is crucial to match sample volume with magnetometer sensitivity to obtain meaningful results. The University of Rochester samples were approximately 3–6 cc in volume, and the Lehigh University samples approximately 11–12 cc in volume. In contrast, the MIT cobble samples were less than 1 cc in volume.

This naturally lowers the starting magnetization of the MIT samples. This weaker initial intensity has severe implications for the definition of characteristic magnetizations which are presented by less than 10% of the total remanence (as is often the case in the JH sediments); specifically these magnetizations are predicted to be below the sensitivity of 2G model 755 SQUID magnetometers.

*3. Absolute magnetometer sensitivity.* Although the Rochester, Lehigh and MIT magnetometers all have the same room temperature bore, only the Rochester system has a high resolution pick-up coil geometry, affording greater sensitivity. A 2G 755 SQUID magnetometer with high homogeneity pick-up coils is adequate to determine the presence of the high unblocking temperature characteristic remanent magnetization in JH quartzite cobbles (as demonstrated by data of the Lehigh lab). However, the high resolution pick-up coil geometry appears necessary to accurately define the ChRM direction.

*4. Practical magnetometer sensitivity.* Differences between the Lehigh University and University of Rochester results can also be attributed to differences in the sample holder blanks (i.e. the Lehigh system utilizes a relatively high mass sample holder and thus has a large associated blank). The MIT system may have higher intrinsic noise due to its operating environment or mode of operation. In particular, the use of an automated sample holder versus single specimen manual measurements can introduce noise. The weakest samples require constant monitoring of drift values during magnetometer usage to obtain meaningful data.

### 4.2. Conglomerate test

With the new paleomagnetic results, we can revisit the conglomerate test (Tarduno and Cottrell, 2013). The conglomerate test significance is defined by finding a value of $R$ for $N$ observations, on the hypothesis of randomness, with a specified probability. If the observed value of $R$ exceeds the critical value $R_o$, the null hypothesis of randomness can be rejected (Watson, 1956). We merge results reported in Tarduno and Cottrell (2013) with new analyses presented here. We exclude results from cobble JC57 because it appears to record a lightning strike and data from JC30 because of directional uncertainty at high unblocking temperatures. We also exclude one sample from the original dataset (JC22) because of its large MAD angle. For the new dataset (Supplementary Table S5) ($N = 28$) (Fig. 10), $R = 4.15$ and is less than $R_o = 8.50$ and we cannot reject the null hypothesis at the 95% confidence level. The observations thus pass the conglomerate test supporting preservation of a primary magnetization. We note that directions from two cobbles [JC1 discussed here and JC5 from Tarduno and Cottrell, 2013] fall close to the expected direction for the 1070 Ma Yilgarn craton field. However, we further note this is not evidence for a pervasive overprint either within a sample or among samples of the JH cobbles. That is, the directions from JC1 and JC5 are defined at high unblocking temperatures; directions at low unblocking are vastly different. When viewed against all the directions, those from JC1 and JC5 are best defined as being drawn from a random distribution.

### 4.3. Magnetic mineral provenance

The sources of the JH sediments are unknown and therefore any provenance information the oxide and sulfide grains we have documented might contain is of potential interest. Spinels have long been used as 'petrogenetic indicators' (Irvine, 1967; Sack and Ghiorso, 1991; Arai, 1992; Barnes and Roeder, 2001) and therefore the JH Cr–Fe spinels merit special consideration. Some prior works near the JH Discovery site, and 0.5 km to the East (Cavosie et al., 2002; Valley et al., 2005) have documented typically low $^{187}Re/^{188}Os$, unradiogenic $^{187}Os/^{188}Os$, and relatively high

zinc contents (1–4 wt%) from Cr–Fe-spinel. The Re–Os data for these grains is consistent with derivation from a normal Eoarchean (3.4 to 3.5 Ga) convecting mantle (S. Shirey, personal communication, 2015). Our Cr–Fe spinels are similar to those reported in the prior work (Cavosie et al., 2002; Valley et al., 2005), although somewhat lower in Mg and Zn. We feel the very low Mg contents (<1 wt%) are atypical of komaiitic sources; such primitive mantle-derived magmas are characterized by Mg-rich spinels (Barnes, 1998).

A more plausible hypothesis is that the low Mg Cr–Fe spinels we have sampled come from a layered intrusion source. One possibility is the Manfred Complex — a once coherent layered anorthosite–gabbro–ultramafic intrusion inferred on the basis of sheared rocks found within the Dugel gneiss of the Yilgarn Narryer Terrane (Myers and Williams, 1985). Anorthosite associated with this complex is about 3.73 billion years old based on U–Pb zircon geochronology [SHRIMP data presented in Kinny et al., 1988]. However, it should be noted that the ultramafic remnants of this complex have not been dated, and therefore exact relationships between the component parts of the Manfred Complex are at present unclear. Furthermore, the Re–Os age constraints of Valley et al. (2005) have been obtained on different chromites than analyzed here. Other anorthosites of the northwest Yilgarn (northwest of Mount Dugal) are 3.5 billion years old (Sylvester et al., 2011), suggesting that other layered intrusions spanning the Eoarchean to Paleoarchean may have been emplaced into the Yilgarn craton, potentially matching the Re–Os age constraints. The Cr–Fe spinels we have recorded include both euhedral and rounded grains, and the contribution of several sources is probable. We suggest that some of the Mg-poor Fe–Cr spinels, Ni-sulfides and pyrrhotites we have sampled form an assemblage coming from a layered intrusion that is one of these sources.

## 5. Conclusions

Through a series of rock magnetic and paleomagnetic measurements, Tarduno and Cottrell (2013) predicted the presence of magnetite in quartzite cobbles of the Jack Hills. This phase is also expected based on the mature nature of the sediments (Eriksson and Wilde, 2010). Our new scanning electron microscope, energy dispersive spectroscopy and electron microprobe analyses conclusively show that magnetite is present as a common phase in the Jack Hills cobbles, confirming the predictions. The presence of magnetite is important because it has high magnetic blocking temperatures and is thus a magnetic mineral with the potential to see through the well-documented greenschist grade metamorphism that has affected the Jack Hills.

The magnetizations isolated at high unblocking temperatures corresponding to magnetite carriers from JH cobble-sized quartzite clasts pass a conglomerate test. The lack of a pervasive overprint at high unblocking temperatures indicates that magnetite in the JH sediments has the potential to preserve pre-depositional remanences, potentially extending the previously oldest known history of the geodynamo (Usui et al., 2009; Tarduno et al., 2010, 2014). This potential has recently been realized through the first Thellier–Thellier paleointensity analyses of JH zircons which reveal magnetizations at unblocking temperatures corresponding to magnetite (Tarduno et al., 2015). We note that Jack Hills zircons could have been reheated after formation but before deposition. Because of slow rates, Pb diffusive losses are irrelevant; instead Tarduno et al. (2015) searched for fluid mediated loss associated with reheating expected in a hydrous crust. For the select zircons bearing paleomagnetic signals, no compelling evidence was seen to support reheating.

An inter-laboratory test confirms the unblocking temperature structure recorded by the JH quartzite cobbles, and the presence of a high unblocking temperature component corresponding to magnetite unblocking temperatures. These comparisons also highlight fundamental considerations for the paleomagnetic measurement of intrinsically weak samples (such as quartzite), which remain a measurement challenge even for laboratories equipped with SQUID magnetometers. Care must be taken to use an appropriate atmosphere during thermal demagnetization and sample volumes must be selected such that magnetization components are greater than magnetometer sensitivity levels after removal of overprints. Magnetometer sensitivity of $\sim 1 \times 10^{-11}$ A m$^2$ is needed to measure some of the weakest JH cobbles.

In addition to magnetite and its oxidized forms (maghemite and hematite), our electron microscope analyses define a range of magnetic mineralogies including Mg-poor Cr–Fe spinel, pyrrhotite (dominantly hexagonal but with some monoclinic phases), and a range of non-magnetic sulfides (pyrite and pentlandite). These magnetic phases can contribute to the complex low unblocking temperature overprint magnetizations recorded by the JH quartzite cobbles, which are dominantly carried by large magnetite and oxidized magnetite grains.

The Cr–Fe spinels and Ni-bearing sulfides indicate an ultramafic source different from the granitoid parent rocks of the JH zircons. The very low Mg contents highlight that the detrital Cr–Fe spinels were not derived from primitive mantle magmas. We suggest that Cr–Fe spinels, Ni-bearing sulfides and some pyrrhotite grains form an assemblage derived from a layered intrusion, remnants of which may be preserved as Paleoarchean enclaves in gneiss of the Yilgarn craton.

## Acknowledgements

## Appendix A. Supplementary material

Supplementary material related to this article can be found online at http://dx.doi.org/10.1016/j.epsl.2016.05.009.

## References

Arai, S., 1992. Chemistry of chromian spinel in volcanic rocks as a potential guide to magma chemistry. Mineral. Mag. 56, 173–184. http://dx.doi.org/10.1180/minmag.1992.056.383.04.

Barnes, S.J., 1998. Chromite in komatiites, 1. Magmatic controls on crystallization and composition. J. Petrol. 39, 1689–1720. http://dx.doi.org/10.1093/petroj/39.10.1689.

Barnes, S.J., Roeder, P.L., 2001. The range of spinel compositions in terrestrial mafic and ultramafic rocks. J. Petrol. 42, 2279–2302.

Burton, B.P., Robinson, P., McEnroe, S.A., Fabian, K., Ballaran, T.B., 2008. A low-temperature phase diagram for ilmenite-rich compositions in the system Fe$_2$O$_3$–FeTiO$_3$. Am. Mineral. 93, 1260–1272. http://dx.doi.org/10.2138/am.2008.2690.

Cavosie, A.J., Valley, J.W., Fournelle, J., Wilde, S.A., 2002. Implications for sources of Jack Hills metasediments: detrital chromite. Geochim. Cosmochim. Acta 66 (Supplement 1), 125.

Chou, Y.M., Song, S.R., Aubourg, C., Song, Y.F., Boullier, A.M., Lee, T.Q., Evans, M., Yeh, E.C., Chen, Y.M., 2012. Pyrite alteration and neoformed magnetic minerals in the

fault zone of the Chi–Chi earthquake ($M_w$ 7.6, 1999): evidence for frictional heating and co-seismic fluids. Geochem. Geophys. Geosyst. 13, Q08002. http://dx.doi.org/10.1029/2012GC004120.

Dunlop, D.J., 1981. The rock magnetism of fine particles. Phys. Earth Planet. Inter. 26, 1–26. http://dx.doi.org/10.1016/0031-9201(81)90093-5.

Dunlop, D.J., Buchan, K.L., 1977. Thermal remagnetization and the paleointensity record of metamorphic rocks. Phys. Earth Planet. Inter. 13, 325–331. http://dx.doi.org/10.1016/0031-9201(77)90117-0.

Dunlop, D.J., Özdemir, Ö., 1997. Rock Magnetism: Fundamentals and Frontiers. Cambridge University Press.

Eriksson, K.A., Wilde, S.A., 2010. Palaeoenvironmental analysis of Archaean siliciclastic sedimentary rocks in the west–central Jack Hills belt, Western Australia with new constraints on ages and correlations. J. Geol. Soc. 167, 827–840. http://dx.doi.org/10.1144/0016-76492008-127.

Irvine, T.N., 1967. Chromian spinel as a petrogenetic indicator, II. Petrologic applications. Can. J. Earth Sci. 4, 71–103. http://dx.doi.org/10.1139/e67-004.

Kadziałko-Hofmokl, M., Delura, K., Bylina, P., Jeleńska, M., Kruczyk, J., 2008. Mineralogy and magnetism of Fe–Cr spinel series minerals from podiform chromitites and dunites from Tapadla (Sudetic ophiolite, SW Poland) and their relationship to palaeomagnetic results of the dunites. Geophys. J. Int. 175, 885–900. http://dx.doi.org/10.1111/j.1365-246X.2008.03933.x.

Kinny, P.D., Williams, I.S., Froude, D.O., Ireland, T.R., Compston, W., 1988. Early Archaean zircon ages from orthogneisses and anorthosites at Mount Narryer, Western Australia. Precambrian Res. 38, 325–341. http://dx.doi.org/10.1016/0301-9268(88)90031-9.

Lagroix, F., Banerjee, S.K., Jackson, M.J., 2004. Magnetic properties of the Old Crow tephra: identification of a complex iron titanium oxide mineralogy. J. Geophys. Res., Solid Earth 109, B01104. http://dx.doi.org/10.1029/2003JB002678.

Li, H.Y., Zhang, S.H., 2005. Detection of mineralogical changes in pyrite using measurements of temperature–dependence susceptibilities. Chin. J. Geophys. 48, 1454–1461. http://dx.doi.org/10.1002/cjg2.794.

Myers, J.S., Williams, I.R., 1985. Early Precambrian crustal evolution at Mount Narryer, Western Australia. Precambrian Res. 27, 153–163. http://dx.doi.org/10.1016/0301-9268(85)90010-5.

Néel, L., 1949. Théorie du traînage magnétique des ferromagnétiques au graus fin avec applications aux terres cuites. Ann. Géophys. 5, 99–109.

Néel, L., 1955. Some theoretical aspects of rock-magnetism. Adv. Phys. 4, 191–243. http://dx.doi.org/10.1080/00018735500101204.

Parker, R.L., 1991. A theory of ideal bodies for seamount magnetism. J. Geophys. Res., Solid Earth 96, 16101–16112. http://dx.doi.org/10.1029/91JB01497.

Pullaiah, G., Irving, E., Buchan, K.L., Dunlop, D.J., 1975. Magnetization changes caused by burial and uplift. Earth Planet. Sci. Lett. 28, 133–143. http://dx.doi.org/10.1016/0012-821X(75)90221-6.

Rasmussen, B., Fletcher, I.R., Muhling, J.R., Gregory, C.J., Wilde, S.A., 2011. Metamorphic replacement of mineral inclusions in detrital zircon from Jack Hills, Australia: implications for the Hadean Earth. Geology 39, 1143–1146. http://dx.doi.org/10.1130/G32554.1.

Rasmussen, B., Fletcher, I.R., Muhling, J.R., Wilde, S.A., 2010. In situ U–Th–Pb geochronology of monazite and xenotime from the Jack Hills belt: implications for the age of deposition and metamorphism of Hadean zircons. Precambrian Res. 180, 26–46. http://dx.doi.org/10.1016/j.precamres.2010.03.004.

Robbins, M., Wertheim, G.K., Sherwood, R.C., Buchanan, D.N.E., 1971. Magnetic properties and site distributions in the system $FeCr_2O_4$–$Fe_3O_4$, ($Fe^{2+}Cr_{2-x}Fe_x^{3+}O_4$). J. Phys. Colloques 32, C1-266–C1-267. http://dx.doi.org/10.1051/jphyscol:1971188.

Sack, R.O., Ghiorso, M.S., 1991. Chromian spinels as petrogenetic indicators thermodynamics and petrological applications. Am. Mineral. 76, 827–847.

Schwarz, E.J., Vaughan, D.J., 1972. Magnetic phase relations of pyrrhotite. J. Geomagn. Geoelectr. 24, 441–458. http://dx.doi.org/10.5636/jgg.24.441.

Sylvester, P., Souders, K., Crowley, J., 2011. The Archean anorthosite–monzogranite magmatic association of the Narryer Gneiss Terrane, Western Australia. Mineral. Mag. 75, 1975.

Tarduno, J.A., Blackman, E.G., Mamajek, E.E., 2014. Detecting the oldest geodynamo and attendant shielding from the solar wind: implications for habitability. Phys. Earth Planet. Inter. 233, 68–87. http://dx.doi.org/10.1016/j.pepi.2014.05.007.

Tarduno, J.A., Cottrell, R.D., 2013. Signals from the ancient geodynamo: a paleomagnetic field test on the Jack Hills metaconglomerate. Earth Planet. Sci. Lett. 367, 123–132. http://dx.doi.org/10.1016/j.epsl.2013.02.008.

Tarduno, J.A., Cottrell, R.D., Davis, W.J., Nimmo, F., Bono, R.K., 2015. A Hadean to Paleoarchean geodynamo recorded by single zircon crystals. Science 349, 521–524. http://dx.doi.org/10.1126/science.aaa9114.

Tarduno, J.A., Cottrell, R.D., Smirnov, A.V., 2006. The paleomagnetism of single silicate crystals: recording geomagnetic field strength during mixed polarity intervals, superchrons, and inner core growth. Rev. Geophys. 44, RG1002. http://dx.doi.org/10.1029/2005RG000189.

Tarduno, J.A., Cottrell, R.D., Watkeys, M.K., Bauch, D., 2007. Geomagnetic field strength 3.2 billion years ago recorded by single silicate crystals. Nature 446, 657–660. http://dx.doi.org/10.1038/nature05667.

Tarduno, J.A., Cottrell, R.D., Watkeys, M.K., Hofmann, A., Doubrovine, P.V., Mamajek, E.E., Liu, D., Sibeck, D.G., Neukirch, L.P., Usui, Y., 2010. Geodynamo, solar wind, and magnetopause 3.4 to 3.45 billion years ago. Science 327, 1238–1240. http://dx.doi.org/10.1126/science.1183445.

Tarduno, J.A., Lowrie, W., Sliter, W.V., Bralower, T.J., Heller, F., 1992. Reversed polarity characteristic magnetizations in the Albian Contessa section, Umbrian Apennines, Italy: implications for the existence of a Mid-Cretaceous mixed polarity interval. J. Geophys. Res., Solid Earth 97, 241–271. http://dx.doi.org/10.1029/91JB02257.

Usui, Y., Tarduno, J.A., Watkeys, M., Hofmann, A., Cottrell, R.D., 2009. Evidence for a 3.45-billion-year-old magnetic remanence: hints of an ancient geodynamo from conglomerates of South Africa. Geochem. Geophys. Geosyst. 10, Q09Z07. http://dx.doi.org/10.1029/2009GC002496.

Valley, J.W., Cavosie, A.J., Shirey, S., Wilde, S.A., 2005. 3.2 to 3.5 Ga Re–Os model ages for detrital chromite from Jack Hills, Western Australia: implications for Pilbara and Yilgarn craton evolution. AGU Fall Meeting Abstracts 21, 08.

Valley, J.W., Cavosie, A.J., Ushikubo, T., Reinhard, D.A., Lawrence, D.F., Larson, D.J., Clifton, P.H., Kelly, T.F., Wilde, S.A., Moser, D.E., Spicuzza, M.J., 2014. Hadean age for a post-magma-ocean zircon confirmed by atom-probe tomography. Nat. Geosci. 7, 219–223. http://dx.doi.org/10.1038/ngeo2075.

Verwey, E.J.W., 1939. Electronic conduction of magnetite ($Fe_3O_4$) and its transition point at low temperatures. Nature 144, 327–328. http://dx.doi.org/10.1038/144327b0.

Watson, G.S., 1956. A test for randomness of directions. Geophys. J. Int. 7, 160–161. http://dx.doi.org/10.1111/j.1365-246X.1956.tb05561.x.

Weiss, B.P., Maloof, A.C., Tailby, N., Ramezani, J., Fu, R.R., Hanus, V., Trail, D., Bruce Watson, E., Harrison, T.M., Bowring, S.A., Kirschvink, J.L., Swanson-Hysell, N.L., Coe, R.S., 2015. Pervasive remagnetization of detrital zircon host rocks in the Jack Hills, Western Australia and implications for records of the early geodynamo. Earth Planet. Sci. Lett. 430, 115–128. http://dx.doi.org/10.1016/j.epsl.2015.07.067.

Wilde, S.A., Spaggiari, C., 2007. The Narryer Terrane, Western Australia: A review. In: van Kranendonk, R.H.S, Martin, J., Bennett, V.C. (Eds.), Developments in Precambrian Geology. In: Earth's Oldest Rocks, vol. 15. Elsevier, pp. 275–304. Chapter 3.6.

Wilde, S.A., Valley, J.W., Peck, W.H., Graham, C.M., 2001. Evidence from detrital zircons for the existence of continental crust and oceans on the Earth 4.4 Gyr ago. Nature 409, 175–178. http://dx.doi.org/10.1038/35051550.

Wingate, M.T.D., Pisarevsky, S.A., Evans, D.A.D., 2002. Rodinia connections between Australia and Laurentia: no "SWEAT", no "AUSWUS"? Terra Nova 14, 121–128. http://dx.doi.org/10.1046/j.1365-3121.2002.00401.x.

Ziemniak, S.E., Castelli, R.A., 2003. Immiscibility in the $Fe_3O_4$–$FeCr_2O_4$ spinel binary. J. Phys. Chem. Solids 64, 2081–2091. http://dx.doi.org/10.1016/S0022-3697(03)00237-3.